ELSEVIER

Catalysis Today 35 (1997) 189–196

CATALYSIS TODAY

The role of the multi-body interaction in the de-NO_x process on solid catalysts investigated by density functional method

Michiyuki Yamadaya, András Stirling [1], Hiroaki Himei, Momoji Kubo, Rajappan Vetrivel [2], Ewa Broclawik [3], Akira Miyamoto *

Department of Molecular Chemistry and Engineering, Faculty of Engineering, Tohoku University, Sendai 980-77, Japan

Abstract

We have performed density functional calculations to investigate the bimolecular $CH_4 + NO_x$ ($x = 1, 2$) and the trimolecular $NO + CH_4 + NO_2$ reactions which can be assumed to occur in the vicinity of an active site on a de-NO_x catalyst. We have shown that the trimolecular reactions can take place very smoothly on a singlet energy hypersurface, while the bimolecular reactions producing unstable radicals are not favorable. We have explained these results with the high energy of the reaction products in the bimolecular reactions and the formation of HNO_x molecules yielding negative stabilization energy in the trimolecular reactions with the extra NO_x molecules which can be considered as spin traps in these processes. We present the geometrical changes together with the electronic changes occurring in the reactions. The significance of this study is that we could demonstrate that the increased concentration of the reaction partners due to an active site of the catalyst allows reactions which otherwise would be unlikely.

Keywords: Density functional calculation; NO_x; Methane activation

1. Introduction

From the global environmental point of view, removal of nitrogen oxides (NO_x) from exhaust gases is significant because compounds are thought to have important role in acid rain and photochemical smog formation or in the ozone layer depletion [1]. The various metal-exchanged zeolites are recent candidates for effective removal of the different compounds (see, e.g., [2–17]). Some of these catalysts, however, not only decompose the gases, but can very successfully reduce them using hydrocarbons (such as methane) even in the presence of excess oxygen [8]. The importance of these reactions cannot be overestimated. In particular, utilizing CH_4 as a reductant is advantageous because methane can be found in every combustion exhaust and this hydrocarbon showed high activity in certain systems [11,13].

Based on the experimental results and the theoretical studies, we can point out the significance of two important roles of a catalyst in a given process: it gathers the reaction partners around the active sites and it lowers the reaction

* Corresponding author.

[1] On leave from the Institute of Isotopes, Hungarian Academy of Sciences, H-1525 Budapest, Hungary.

[2] Present address: Catalysis Division, National Chemical Laboratory, Pune 411088, India.

[3] Present address: Institute of Catalysis, Polish Academy of Sciences, Cracow PL-30239, Poland.

PII S0920-5861(96)00127-7

barriers. As for the former, this is an indispensable element for an effective process, while the latter is very important in the reaction rate increase. Utilization of these advantages is therefore very important in catalyst research. To demonstrate and analyze the importance of these effects in the de-NO_x process, we have examined the reactions of NO and NO_2 with methane. In this study, we focused on the consequences of the concentration (or collecting) effect of an active site, which means that in the vicinity of the active site, the concentration of the reaction partners is higher than in the farther regions and the increased concentration opens new reaction routes which otherwise are not possible. In this study, we followed bi- and trimolecular reaction paths which can be assumed near the active site. While in gas phase the energetically favorable reaction is

$$CH_4 + NO_x \rightarrow CH_3 + HNO_x \quad (1)$$

since the NO_x molecule can more easily form a bond with the outer H atoms than the inner carbon atom, in the vicinity of the active site of a de-NO_x catalyst, reactions which produce CH_3NO_x species can also take place because, for instance, CH_3NO_2 molecules can be supposed as an active intermediate in, e.g., Cu-MFI [18]. It is important to note that we could not find similar theoretical or experimental studies published in the last fifteen years. In addition, experimental investigations on the reaction of NO_x molecules with hydrocarbon radicals (like methyl radical) can only be found [19,20].

We chose the density functional method [21,22] for our investigations. This method is not as expensive computationally as the traditional Hartree–Fock based correlation methods, but it can take into account the electron correlation which is very important for systems which contain high electronegativity elements like oxygen and nitrogen. This approach has also been proved to be very effective for similar systems [23,24]. In addition, when we describe chemical reactions, the electron correlation cannot be neglected.

The organization of our paper is the following: after the computational details, we discuss the reliability of our models, analyze the bimolecular $CH_4 + NO_x$ reactions and compare them with the trimolecular $CH_4 + NO + NO_2$ reactions. In the last part, we would like to summarize the conclusions which can be drawn from the results.

2. Computational details

All density functional (DF) calculations described here were performed using the self-consistent Kohn–Sham procedure [22] as implemented in the DMol program package [25] of Biosym Technologies, Inc. (The description of the technical details is given in [26] and [27].) The calculations were carried out at two levels of the approximations for the exchange-correlation potential. We used local density approximation with the Janak–Moruzzi–Williams (JMW) functional [28] for the energy curve calculations and geometry optimizations. In order to calculate accurate energy values, we applied the Becke–Lee–Yang–Parr (BLYP) non-local functional [29] for the optimized geometry obtained from local calculations. We used double-numerical + polarization functions (DNP) basis set for all the calculations. This set is of Gaussian 6-31G** quality, a standard basis set in quantum chemistry. The geometry optimizations were performed with the aid of analytical gradients using the Broyden–Fletcher–Goldfarb–Shanno (BFGS) algorithm [30]. We accepted the optimized geometries when the norm of the gradient vector was less than 0.001 a.u. The calculated energy differences are not free from the basis set superposition error, but this error is minimized by the quality of the basis set used in the calculations [26].

3. The models

In this paper, we theoretically investigate bi- and trimolecular reactions between CH_4 and

NO_x molecules, which can be assumed to take place on the active site of an appropriate catalyst. However, we do not explicitly take into account the active site. What we therefore calculate are apparently gas-phase reactions, but we emphasize again, that these types of reactions are either not the energetically favorable or not the likely reactions in gas phase. Notwithstanding, experimental findings of the CH_3NO_x species [18] make these reactions probable when using different catalysts, although there is no unanimously accepted reaction mechanism for their formations. In order to suggest possible reaction steps which can explain the unique role of the active site in the de-NO_x process, we calculated different reaction paths and their energy profiles for these reactions. From these curves and other results, such as the geometries and the electronic structure changes, we can understand the reaction mechanism and the importance of the active sites.

4. Bimolecular reaction of CH_4 and NO_x ($x = 1, 2$)

Although in gas phase reaction (1) seems to be favorable, in the catalytic de-NO_x process, the CH_3 intermediates also have an important role [18]. An obvious assumption is that bimolecular reactions between CH_4 and NO_x yield these species. In order to describe these reactions, we performed the following series of calculations: the reaction energy profile for both the $CH_4 + NO$ and the $CH_4 + NO_2$ reactions was estimated with respect to the carbon–nitrogen distance, while all the other atomic positions were fully optimized at the local exchange-correlation level. We also determined the non-local energy curves using the local geometries for every carbon–nitrogen distance which we consider as more reliable than the local curves. The reason for this procedure is that it is a well-known fact, that while the local approximation produces acceptable geometries, the non-local corrections are indispensable for the energy and energy difference estimation [31]. Nevertheless we present both the local and non-local results to demonstrate the differences.

Table 1 shows the calculated energies for the two different bimolecular reactions, while Fig. 1 connects them with the corresponding geometries. The energies represent the relative or stabilization energies of the systems compared to the starting point, so the horizontal 'zero' line corresponds to the isolated gas phase $CH_4 + NO_x$ molecules. We can see that first we obtained a large energy barrier for the transition state and then a local minimum point for both reactions. These high energy barriers clearly show that the bimolecular reactions are energetically not favorable, both at the local and at non-local levels.

From the calculations, we have obtained the following two reaction equations:

$$CH_4 + NO \rightarrow CH_2NO + H_2 \quad (2)$$

$$CH_4 + NO_2 \rightarrow CH_3NO_2 + H \quad (3)$$

It is interesting to see that in Eq. (2), H_2 is formed. This is very unusual under the experimental conditions and this result makes this reaction very unlikely. For the sake of comparison, we analyzed both reactions.

From Fig. 1, we can understand the main steps of the (2) and (3) reactions. It appears that the NO forms a shorter bond with the methylene group and also the C–N distance in the CH_4–NO system is shorter in the transition state than for the CH_4–NO_2 system. In the transition state of Eq. (3), from the arrangement of the H atoms, we can see the two, which will form the H_2 molecule, while in the transition state of (3)

Table 1
Relative energy values (in kcal/mol) of the transition and final states in the bimolecular reactions

	$CH_4 + NO$ (Eq. (2))		$CH_4 + NO_2$ (Eq. (3))	
	Local	Non-local	Local	Non-local
Transition state	+61.9	+88.0	+45.5	+64.3
Final state	+14.4	+25.1	+32.8	+49.4

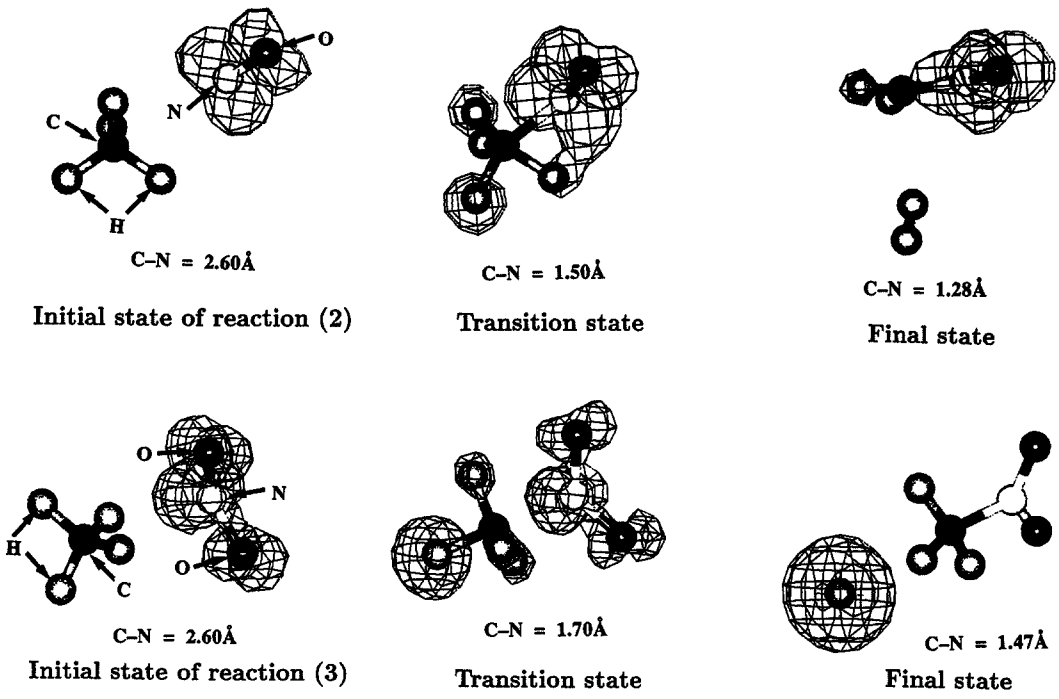

Fig. 1. The geometrical and electronic changes during the bimolecular reactions.

three of the H atoms and the carbon atom form a plane which indicates a strong similarity to the organic substitution reactions. We can also observe that after the transition states the H_2 molecule or the outermost hydrogen atom separated completely in the $CH_4 + NO$ and the $CH_4 + NO_2$ systems, respectively, while the new, strong C–N bonds formed. In order to understand why the bimolecular reactions are *not* favorable, let us turn to Fig. 1 again, which presents the spin density of the relevant configurations for both reactions. The spin density ($\rho^S(\mathbf{r})$) is the difference of the densities of α and β electrons:

$$\rho^S(\mathbf{r}) = \rho^\alpha(\mathbf{r}) - \rho^\beta(\mathbf{r}) \quad (4)$$

It is well known that the nitrogen oxides which contain one nitrogen atom are doublets, that is they have an unpaired electron on their highest (singly) occupied orbital. This single electron generates a spin-density around the molecule which more or less shows the shape of the highest occupied orbital. Following the changes of the spin density, we can analyze the forming and breaking bonds as well as the stability of the different configurations, since this excess spin cannot disappear during the reactions. It can easily be seen that during the reactions the original spin density was 'transferred' from the NO_x molecule to the formed CH_2NO molecule and to the H atom, while in the transition state it covers all the CH_4–NO_x systems. The spin density of the CH_2NO molecule, however, is mainly localized on the NO part of the molecule which indicates that the single electron does not take part in the C–N bond formation.

Comparison between the energy profiles of the reactions of CH_4 with NO or NO_2 reveals similar trends for these processes with similar energy curves. Table 1 summarizes the most important energy values for the curves. From these values, we can see only slight differences between the two reactions: the new C–N and H–H bonds can stabilize the $CH_2NO + H_2$ system in a higher degree than the C–N bond alone does for the $CH_3NO_2 + H$ system (+25 and +50 kcal/mol, respectively, at the non-local

level), although, for the latter system, the energy barrier is lower. Another interesting difference between the two systems is that the local minimum point for the CH_4–NO system corresponds to a somewhat smaller C–N bond distance (1.30 Å) than the minimum C–N distance in the $CH_4 + NO_2$ system (1.47 Å), but the calculated C–N bond lengths are in good agreement with those of the calculated gas-phase (isolated) CH_2NO and CH_3NO_2 molecules. This means that the reaction products are well separated and do not perturb each other.

Now it is easy to understand why we could not obtain negative stabilization energies: localizing the single electron in a high energy radical or around a proton produces a much less stable system than having an electron on a large NO_x orbital together with the stable CH_4 molecule; moreover, this instability cannot be compensated by the new C–N and H–H bond formations. Nevertheless, the most important common feature of the two bimolecular reactions is the presence of a high energy barrier followed by a local minimum point along the C–N bond formation curves. This minimum structure, however, corresponds to a less stable state as compared to the initial, well-separated CH_4–NO_x systems due to the new radical formation.

5. Trimolecular NO + CH_4 + NO_2 reactions

It is evident, that if we can stabilize the forming radicals in statu nascendi, we can obtain a more stable state for our reaction system. In the vicinity of a catalytic active site we can assume another NO_x molecule due to the gathering effect of the catalyst. This molecule can be an ideal spin trap, considering the fact that the NO_x molecule itself is a radical.

Certainly, we can suppose different combinations for this trimolecular reaction. We have investigated two of them with the stoichiometry of $CH_4 + NO + NO_2$ because this stoichiometry has been accepted as an important combination of the molecules in the de-NO_x processes [13]. The calculation procedure was similar to the bimolecular calculations. At different, fixed C–N^1 bond distances, where N^1 is the nitrogen atom of the NO_x molecule which will form the C–N bond, we calculated the optimum geometry as well as the stabilization energy of the total system including the other NO_x molecule. The initial N^2–C distance, where N^2 is the nitrogen atom of the trapping NO_x molecule, was more than 3.0 Å and the three central N, C, and N atoms lay in line. However, there is an essential difference between the bi- and trimolecular reactions. The bimolecular reactions take place on a doublet energy hypersurface, whereas the trimolecular reactions need a transition between triplet and singlet states. This is so because after the excess spin is trapped by a NO_x molecule in the trimolecular process, no uncompensated spin can be found in our system, while at the starting point, both NO_x molecules have a single, unpaired electron on their highest (singly) occupied orbitals, which can be interpreted as a triplet state. In our calculations, the triplet–singlet mixing (transitions) occurred at larger (> 2.2 Å) C–N^1 distances, which means that we could analyze the singlet energy curves only.

From the calculations, we obtained the energies and the geometrical changes presented in Table 2 and Fig. 2, respectively. From these we could deduce the following routes:

$$N^2O_2 + CH_4 + N^1O \rightarrow CH_3N^1O + HN^2O_2 \quad (5)$$

$$N^2O + CH_4 + N^1O_2 \rightarrow CH_3N^1O_2 + HN^2O \quad (6)$$

Table 2
Relative energy values (in kcal/mol) of the transition and final states in the trimolecular reactions

	$NO_2 + CH_4 + NO$ (Eq. (5))		$NO + CH_4 + NO_2$ (Eq. (6))	
	Local	Non-local	Local	Non-local
Transition state	+4.5	+22.9	+2.7	+18.9
Final state	−31.5	−10.1	−26.2	−8.4

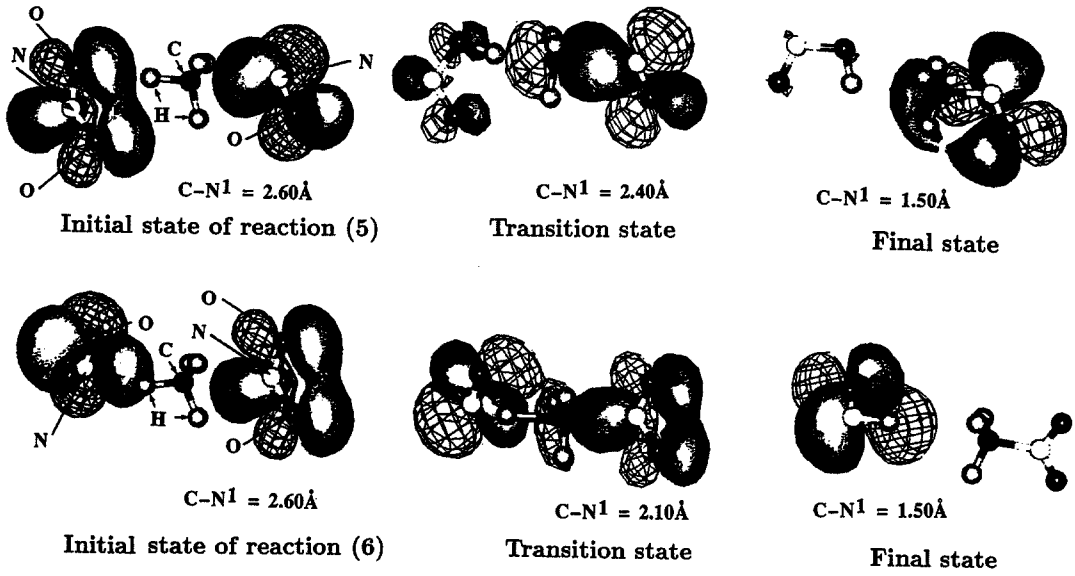

Fig. 2. The geometrical and electronic changes during the trimolecular reactions.

In reaction (5), the NO_2 plays the role of the spin trap, whereas in reaction (6), the NO molecule will trap the excess spin. (The superscript 1 or 2 indicates the different role of the nitrogen atoms, similarly to the previous paragraph.) We note that no CH_2NO formation occurs in these processes.

Table 2 shows the predicted energies at both the local and non-local levels for reactions (5) and (6). It can easily be ascertained from these values that both trimolecular reactions can take place, resulting in negative stabilization energies after small energy barriers. The data presented here clearly illustrate the difference between the bi- and trimolecular reactions. Since the trimolecular reactions do not produce free radicals, these processes are energetically favorable (with about -8–10 kcal/mol non-local stabilization energy). Moreover, the height of the energy barriers for the reactions is very small (around $+20$ kcal/mol at the non-local level), which makes these reactions theoretically very likely.

Fig. 2 shows the most important configurations similarly to Fig. 1. A close inspection of the geometry data reveals that the trimolecular reactions run similarly to the bimolecular (3) process; namely, they reflect a radical substitution mechanism, but in this case the leaving H atom forms a new bond consecutively with the spin-trap NO_x molecule. This step is responsible for the negative stabilization energies. The geometry of the formed CH_3NO_x molecules is in accordance with the theoretical gas phase geometry for cases of both NO and NO_2. We note that in the minimum points the N^2–C distances are larger than 4 Å, which means that after the reaction, the reaction products are completely separated.

In order to illustrate the electronic changes during the reactions, we also present the molecular orbitals in Fig. 2. This figure shows the highest occupied molecular orbital (HOMO) for the transition states and the final configurations, together with the two singly occupied molecular orbitals (SOMOs) for the initial geometries. (In the trimolecular cases, no spin density can be found after the reactions reached the singlet energy hypersurface so we cannot use the spin density plots for analysis.) From this figure we can understand how the two SOMOs combined with the CH_4 orbitals and form new lower lying orbitals and HOMOs for the CH_3NO and the HNO molecules in the reaction (5) and (6),

respectively. (It is interesting to note that the HOMO orbitals belong to the molecules which formed from the NO molecule in both cases.) We can also see that, in the transition state, the leaving H atom is overlapping with the NO_2 $5A_1$ orbital (in reaction (5)) or with the NO π^* orbital (in reaction (6)), which is essential for the new N–H bond formation. Of course, the lower lying orbitals also take part in the formation of the new molecules, but the highest orbitals play the most interesting role in the catalytic processes.

6. Conclusions

We have examined bi- and trimolecular reactions which we assumed to take place on the active site of a de-NO_x catalysts, due to its concentrating effect, in order to account for the formation of some experimentally found species and experimental stoichiometry. The density functional calculations revealed that the trimolecular reactions can run smoothly, despite the fact that this type of reaction is very unlikely in gas phase, whereas the bimolecular reactions were proved to be unfavorable energetically. The key result of this study was that the formation of a high energy radical (CH_2NO molecule and H atom in our cases) is responsible for the high energy barrier and positive stabilization energy, while in the trimolecular reactions, the leaving H atom can form a stable bond with any NO_x molecule. This simultaneous bond breaking and forming eliminates the high energy barrier and can stabilize both the transition state and the final state. Our results therefore suggest that, if we can realize the high concentration of the NO_x and CH_4 molecules, we can carry out such trimolecular reactions. In addition, another outcome is that we can assume trimolecular or quasi-trimolecular reactions occurring on a de-NO_x catalyst when CH_3NO_x intermediates are found. Certainly, we have to keep in mind that one of the most important effects of a catalyst is that it can modify (lower) the energy barriers of a particular process, or it can open a new reaction route for this process. We therefore think that our calculated energy barriers can be considered as an upper bound for the real reaction hindrances and the reaction heats are very approximate. It follows that these results are highly qualitative, but still provide important information about the details of the reactions.

Similar studies have not been carried out to the best of our knowledge. We think that our results may provide new insight into the de-NO_x processes. It is also hoped that our proposed mechanism can serve as an initial point for further studies. Some possible extensions can be the inclusion of the active site orbitals into the calculations or description of other possible reactions with or without the active sites, like reactions of NO_x molecules with other hydrocarbon molecules. We believe that our approach will further stimulate theoretical and experimental investigations.

References

[1] J.N. Armor, Appl. Catal., B1 (1992) 221.
[2] S. Sato, Y. Yu-u, H. Yahiro, N. Mizuno and M. Iwamoto, Appl. Catal., 70 (1991) L1.
[3] M. Iwamoto, H. Yahiro, Y. Mine and S. Kagawa, Chem. Lett., (1989) 213.
[4] M. Iwamoto, H. Furukawa, Y. Mine, F. Uemura, S. Mikuriya and S. Kagawa, J. Chem. Soc. Chem. Commun., (1986) 1272.
[5] M. Iwamoto, H. Yahiro and K. Tanda, Stud. Surf. Sci. Catal., 44 (1989) 219.
[6] M. Iwamoto and H. Yahiro, Catal. Today, 22 (1994) 5.
[7] M. Kishida, T. Tachi, H. Yamashita and H. Miyadera, Shokubai, 34 (1992) 148.
[8] Y. Li and J.N. Armor, Appl. Catal., B1 (1992) L31.
[9] Y. Li and J.N. Armor, Appl. Catal., B2 (1993) 239.
[10] Y. Nishizawa and M. Misono, Chem. Lett., (1993) 1295.
[11] K. Yogo, M. Ihara, I. Terasaki and E. Kikuchi, Chem. Lett., (1993) 229.
[12] Y. Li and J.N. Armor, J. Catal., 145 (1994) 1.
[13] E. Kikuchi and K. Yogo, Catal. Today, 22 (1994) 73.
[14] M. Misono and K. Kondo, Chem. Lett., (1991) 1001.
[15] Y. Kintaichi, H. Hamada, M. Tabata, M. Sasaki and T. Ito, Catal Lett., 6 (1990) 239.
[16] G. Mabilon and D. Durand, Catal. Today, 17 (1993) 285.
[17] T. Ishihara, M. Kagawa, Y. Mizuhara and Y. Takita, Chem. Lett., (1992) 2119.

[18] M. Iwamoto and H. Takeda, in Workshop on Environmental Catalysis, The Role of IB Metals, Osaka, Japan (1995).
[19] A. Lifshitz, C. Tamburu, P. Frank and T. Just, J. Phys. Chem., 97 (1993) 4085.
[20] H. Yang, V. Lissianski, J.U. Okoroanyanwu, W.C. Gardiner and K.S. Shin, J. Phys. Chem., 97 (1993) 10042.
[21] P. Hohenberg and W. Kohn, Phys. Rev. B, 136 (1964) 864.
[22] W. Kohn and L.J. Sham, Phys Rev. A, 140 (1965) 1133.
[23] J.M. Seminario and P. Politzer, Int. J. Quantum Chem., S26 (1992) 497.
[24] A. Stirling, I. Papai, J. Mink and D.R. Salahub, J. Phys. Chem., 100 (1994) 2910.
[25] DMol version 2.3.5 San Diego: Biosym Technologies, 1993.
[26] B. Delley, J. Phys. Chem., 92 (1990) 508.
[27] B. Delley, J. Phys. Chem., 94 (1991) 7245.
[28] V.L. Moruzzi, J.F. Janak and A.R. Williams, Calculated Electronic Properties of Metals Pergamon, New York, 1978.
[29] (a) A. Becke, J. Chem. Phys., 88 (1988) 2547; (b) C. Lee, W. Yang and R. G. Parr, Phys. Rev. B, 37 (1988) 786.
[30] H.B. Schlegel, in K.P. Lawley (Editor) Ab initio Methods in Quantum Chemistry, Vol. I, Wiley, New York, 1987.
[31] T. Ziegler, Chem. Rev., 91 (1991) 651.